



Analysis of Concentrations of Coarse Fraction Particle Levels (PMCO) in Mexico City with Probability Distribution Functions

M. Sc. Zenteno Jiménez José Roberto

M. Sc. Antonio Barba Gutiérrez

*Geophysical Engineering, National Polytechnic Institute, Mexico City,
ESIA-Ticóman Unit, Mayor Gustavo A. Madero*

E-mail: jzenteno@ipn.mx

E-mail: tono1347@outlook.com

Abstract: The study includes an analysis of data from 2011 to 2018, it was proposed to obtain the best or best Probability Distribution Functions that Model PMCO Concentrations in Mexico City, using the following PDF, Gama Distribution Function, Function of Distribution Extreme Value Distribution and Nakagami Distribution Function, to obtain the estimators, the Maximum Probability and Moments Method was used and aided by the Matlab 2017 program, for the evaluation of the forecast model, RMSE, Determination Coefficient, Prediction Approach and Index were used Approach, in turn an analysis is made to observe its trend within the period using the Bayesian Point Change Detection method to observe the most notable variations of the trend, the database used is from the official air page From Mexico City.

Keywords: Particulate Material Coarse Fraction, Probability Distributions, Adjustment Indicators.

The Coarse Fraction Particles of Mexico City Trend 2011 – 2018

Suspended particles present in the air are divided into different categories depending on their size (aerodynamic diameter). Coarse particles are airborne particles that are relatively large in size and are mainly produced by disintegration of even larger particles. Dust, pollen, spores, fly ash and fragments of plants and insects are examples of coarse particles. The coarse particles have an aerodynamic diameter between 2.5 and 10 μm (PM_{10-2.5}).

Given the stochastic nature of atmospheric processes, air pollutant concentrations can be treated as random variables with measurable statistical properties. If certain conditions are the statistical characteristics of pollutant concentrations, they can be described by probability density functions. Probability density functions (pdf) have been widely used in recent years in a variety of applications, where data smoothing,

Interpolation or extrapolation is needed (Wilks, 1995). Specifically, in the atmospheric sciences the most characteristic applications include the approximation of the frequency of exceeding the critical concentration levels and the estimation of the emission reduction, required for the objective air quality standard (Georgopoulos and Seinfeld, 1982; Abatzoglou et al., 1996; Burkehardt et al., 1998; Morel et al., 1999).

Atmospheric Pollution by Particles

Due to the problem of air pollution, it has become essential both to monitor and measure various chemical components that, due to their emission into the air, already represent a complex problem even with climatic ranges and some with direct effects on human health.

Among the air pollutants with the greatest harmful effect are hydrocarbons, some sulfur and nitrogen compounds, monoxide and carbon dioxide, and those that are part of this work refer to PM₁₀ and PM_{2.5} particles, which are called coarse and fine particles. Due to their micrometric size they are imperceptible to people but they enter the respiratory system very easily causing several inherent diseases.

To know the sources of pollutants in Mexico, the "Emissions Inventory" was created by SEMARNAT, which is updated every three years.

There are three main types of air pollutants.

1.- Those that are emitted directly into the atmosphere as a result of combustion or other industrial processes called primary pollutants such as sulfur dioxide (SO₂), carbon monoxide (CO), Hydrocarbons (HC), some solvents, lead (Pb) and suspended particles (PS).

2.- Primary pollutants already in the atmosphere can react chemically and produce so-called secondary pollutants such as O₃, NO₂, and some types of particles.



3.- The greenhouse gases (G.E.I.) causing global warming such as CO₂, CH₄ and nitrous oxides as the most important.

Due to their emission, the area sources together with the mobile sources are those that provide the greatest amount of respirable fraction particles to the atmosphere, which are PM₁₀, PM_{2.5} and black carbon (CN).

Apart from the classification of particles as primary and secondary, a classification by size is also used, which although they can take many forms, their aerodynamic diameter is considered, which is the particle size as a spherical particle of unit density under conditions of temperature, pressure and existing humidity. This concept allows to determine the transport, the processes of removal in the air and surfaces as well as the trajectory of the particles within the human respiratory system.

Originally, the air quality indicator referring to the particles was only the "Total Suspended Particles" (PST). Subsequently, the studies focused on PM₁₀ (thick breathable) particles and more recently in the PM_{2.5} (fine) range. up to PM₁₀, and even ultra-thin calls smaller than 1 micrometer.

Both fine and coarse particles can be primary, however, in general, fines are considered secondary. The following table summarizes some characteristics according to the type of particles.

Características	Tipo de Partículas		
	Ultra finas PM _{0.1}	Finas (≤PM _{2.5})	Gruesas (PM _{2.5} -PM ₁₀)
Solubilidad	No están bien caracterizadas	Muy solubles	Muy insolubles y no higroscópicas
Vida media atmosférica	Minutos a horas	Días a semanas	Minutos a horas
Proceso de remoción	Crece en la moda de acumulación Se difunden en gotas de lluvia y otras superficies	Formación de nubes y lluvia Precipitación seca	Precipitación seca Eliminación por gotas de lluvia
Distancia de transporte	De menos de uno a decenas de kilómetros	De cientos a miles de Kilómetros	De menos de un Kilómetro a decenas de Kilómetros (de cientos a miles de Kilómetros en tormentas de arena para la fracción de tamaños pequeños)

Figure 1. Source: EPA 2009, "Integrated Science Assessment for Particulate Matter"

All types of particles vary in their shape, size, chemical composition and permanence in the atmosphere as they can be spherical, ellipsoidal, cubic or irregular shapes including geometric and fractal, and with the above you must determine their optical properties that play a significant role in the radioactive balance of the planet in its interaction with solar energy.

The chemical composition of the particles is very diverse and depends on both the source and the mechanism of formation in the atmosphere.

Usually in the coastal regions the particles are formed by sodium chloride (NaCl) while those of geological origin are formed by ferrous oxide (FeO), ferric oxide (Fe₂O₃), calcium, silica and aluminum.

In turn, the INE conducted a study in 2009 on the spatial variability, composition and toxicity of the particles in the CDMX, finding that calcium is the majority element in PM₁₀ while sodium, sulfur and calcium are major elements in PM_{2.5} and in this same fraction the sulfate ions (SO₄) are the most present.

Another study carried out in the CDMX within the "Miracle" campaign where the composition of the contaminating particles was analyzed was that the greatest contribution is made by organic compounds from the burning of biomass and urban sources generating primary and secondary particles, followed by nitrates, sulfates and ammonium compounds.

The particles are removed from the atmosphere by different processes such as sedimentation and rainfall. On the other hand, the residence time in particles larger than 20 micrometers remain for several hours while those of 2 to 3 micrometers the permanence interval is 2 to 4 days and those of 0.1 to 1 micrometer remain from a few days to weeks and They are removed almost exclusively by rain. Carbon and organic particles are difficult to wet, so before being removed by precipitation they go through an oxidation period, which results in longer residence times with respect to inorganic particles such as sulfates.

According to data published by the Secretariat of the Environment of the City of Mexico in the Inventory of Emissions of the City of Mexico 2016. General Directorate of Air Quality Management, Directorate of Air Quality Program and Inventory of Emissions City of Mexico. September 2018. The transport sector is the main emitter of particles of the City of Mexico because it contributes with 53% of the emissions of PM₁₀ and 56% of PM_{2.5} coming mostly from heavy units that use diesel and private cars to gasoline.

On the other hand, the environmental aspect of air pollution has a direct impact on health in both developed and developing countries.



It is estimated that air pollution in both cities and rural areas was the cause of 4.2 million premature deaths per year worldwide and this mortality is due to the exposure of particles of 2.5 microns or less causing cardiovascular disease, respiratory and cancer. This according to the publication of the World Health Organization of May 2, 2018.

To concentrate some data on particle size and its impact on health, the following table is shown.

Tamaño de partícula (µm)	Región donde puede ocurrir la penetración
11	Capturadas en orificios nasales; no penetran en la parte baja del tracto respiratorio
7 > 11	Pasaje nasal
4.7 - 7	Región de la laringe
3.3 - 4.7	Tráquea y región primaria bronquial
2.1 - 3.3	Región bronquial secundaria
1.1 - 2.1	Región bronquial terminal
0.65 - 1.1	Bronquiolos
0.43 - 0.65	Alveolos

Figure 2. Source: Borja- Aburto V.H “Evaluation of Health Effects of Pollution”

Based on the previous brief information regarding the types of particles mentioned as well as their contaminating effects on the environment and on health, the statistical study of this work is of utmost importance in order to learn more about their behavior in the atmosphere and more specifically in Mexico City as a great support for the necessary and urgent political, technical and regulatory decisions of the corresponding institutional instances.

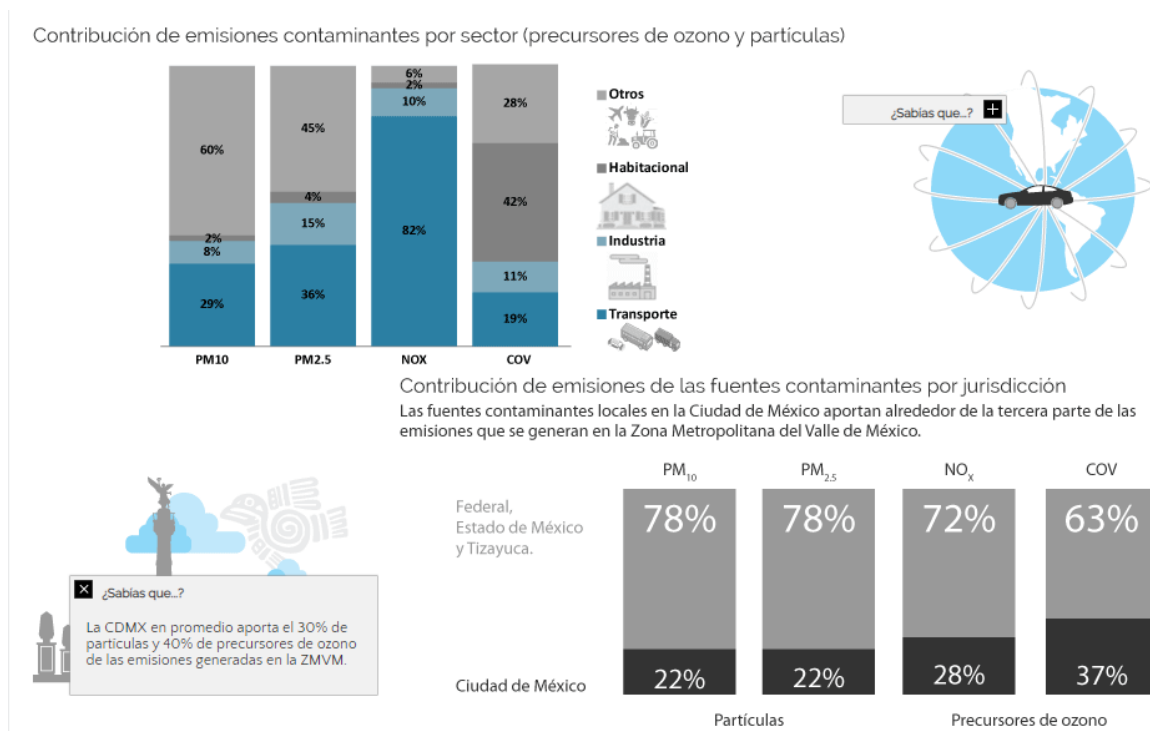
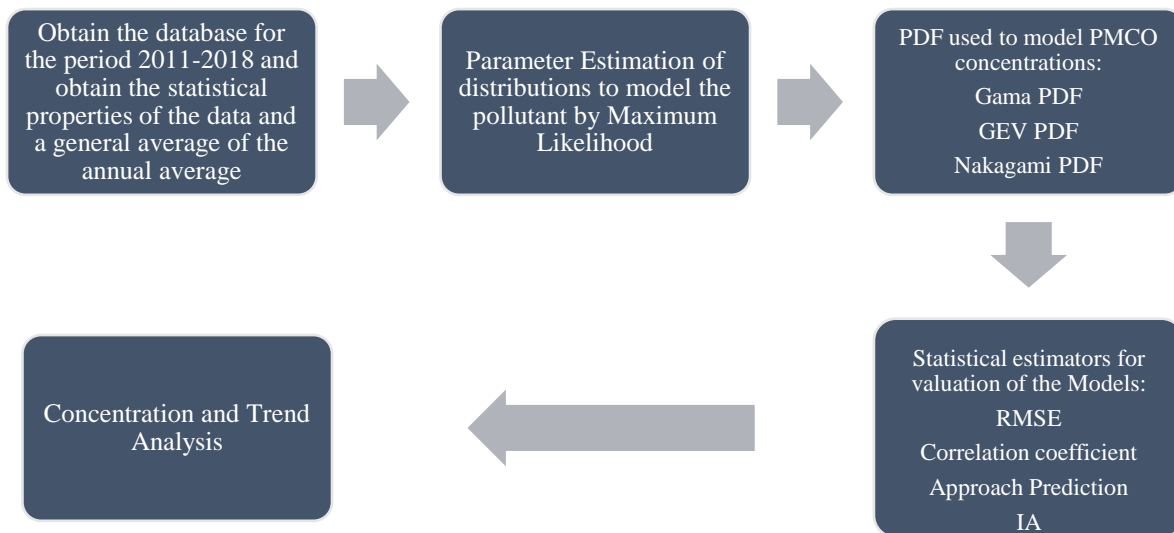


Figure 3. Contribution of particulate pollutant emissions in Mexico City

(Source: <http://www.aire.cdmx.gob.mx/default.php>)



Functions of Probability Distribution and Methodology



Three probability distribution functions were used, which are the Gama Distribution function, the GEV Distribution function and the Nakagami Distribution function.

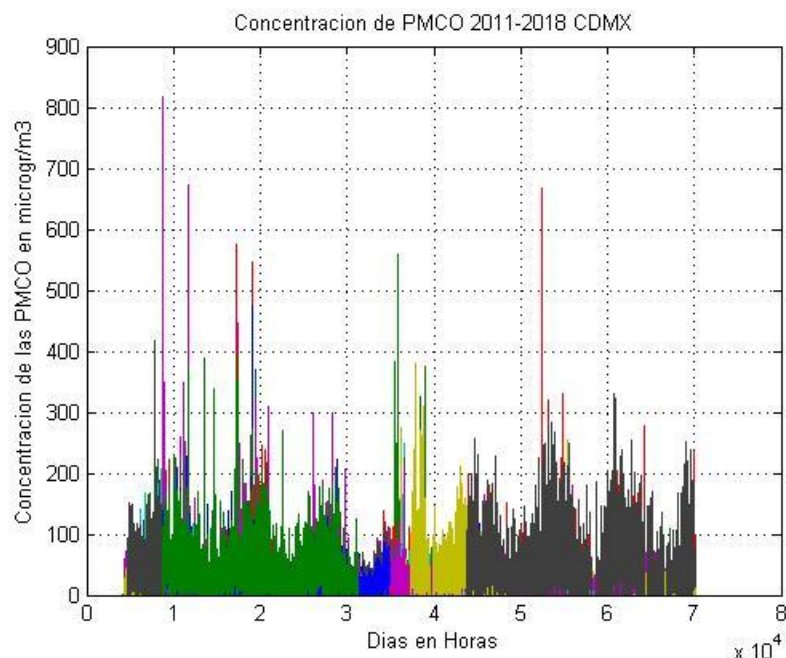


Figure 4. Temporary Concentration Series of PMCO in $\mu\text{gr}/\text{m}^3$ Mexico CityTrend 2011-2018 in hours

Table1. Probability Distribution Functions and their Parameters

Distribution	Probability Density Function	Parameters
GEV	$f(x) = \left(\frac{1}{\sigma}\right) \exp \left(- \left((1+kz)^{-\frac{1}{k}} \right) (1+kz)^{-1-\frac{1}{k}} \right)$ $z = \frac{x - \mu}{\sigma}$	K shape σ scale μ location



Nakagami	Defined in a semi-infinite interval, usually $[0, \infty)$ $f(x) = \left(\frac{2\mu^\mu}{\Gamma(\mu)\Omega^\mu} \right) x^{2\mu-1} \exp\left(-\frac{\mu}{\Omega}x^2\right)$	Ω control extension μ shape
Gama	$f(x) = \frac{\text{Beta}^{\text{alfa}}}{\Gamma(\text{alfa})} x^{\text{alfa}-1} e^{-\text{Beta}x}$	$\text{Beta} = \frac{\sum x_i^2}{\sum x_i} - \frac{\sum x_i}{N}$ $\text{Alfa} = \frac{(\sum x_i)^2}{N \sum x_i^2 - (\sum x_i)^2}$

Study Área of Mexico City

Mexico City in its geographical location is located in a closed or almost closed basin, which in all directions is north, south, east or west, borders a mountain range or mountain pass, which the highest altitude is with the volcanoes to the east the Popocatepetl and the Iztaccihualt, which the wind circulation and the dispersion of pollutants makes it difficult, both for suspended particles and for other pollutants.

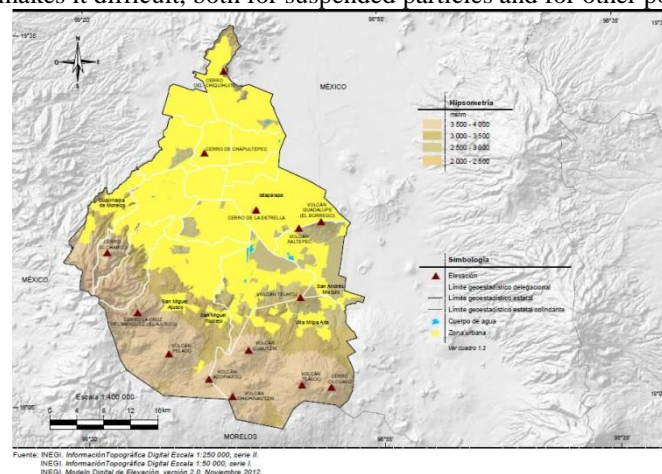


Figure 5. Relief of Mexico City (Source: <https://www.paratodomexico.com/>)

Statistical Adjustment Estimators

The deviation indicators of a group of data in relation to a model can be used to assess the goodness of fit between the two. Among the most common indicators are the following: RMSE, MAE, NRMSE, CV-MRSE, SDR, and R^2 . Those that were used to determine the distribution that best fit the data. They are the mean square error (RMSE), the approximation index (IA), prediction accuracy (AP) and coefficient of determination (R^2) Table 2 gives the equations for the adjustment indicators that have been used by Lu (2003) and Junninen et al. (2002).

Table 2. Adjustment Estimator

Estimator	Equation
Error Measures	
Root Mean Square Error	$RMSE = \sqrt{\left(\frac{1}{N-1} \right) \sum_{i=1}^N (P_i - O_i)^2}$
Accuracy Measures Coefficiente of Determination	$R^2 = \left(\frac{\sum_{i=1}^N (P_i - P)(O_i - O)}{NS_p S_o} \right)^2$
Accuracy Measures Prediction Accuracy	$AP = \frac{\sum_{i=1}^N (P_i - O)^2}{\sum_{i=1}^N (O_i - O)^2}$
Accuracy Measures Index of Accuracy	$IA = 1 - \frac{\sum_{i=1}^N (P_i - O_i)^2}{\sum_{i=1}^N (P_i - O + O_i - O)^2}$



Notation: N = Number of Observations, P_i = Predictive Values, O_i = Observed Values, P = Average of Predicted Values, O = Average of Observed Values, Sp = Standard Deviation of Predicted Values, So = Standard Deviation of Values Observed.

Statistical Description of the Data

Mean = $27.9 \mu\text{gr}/\text{m}^3$

Standard Deviation = $9.33 \mu\text{gr}/\text{m}^3$

Variance = $76.68 \mu\text{gr}/\text{m}^3$

Mode = $10.07 \mu\text{gr}/\text{m}^3$

Median = $12.28 \mu\text{gr}/\text{m}^3$

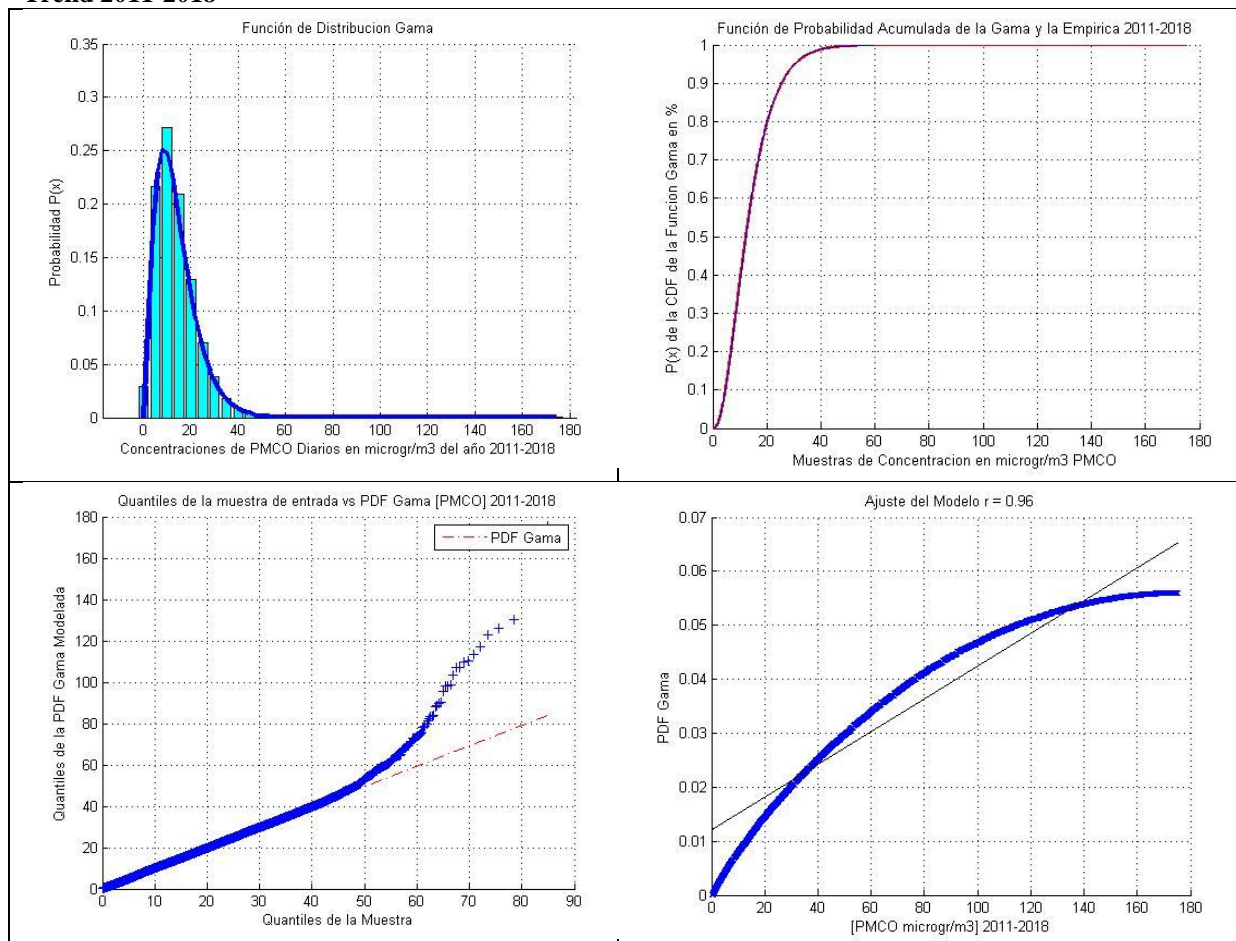
Máx = $175 \mu\text{gr}/\text{m}^3$

Mín = $0.0714 \mu\text{gr}/\text{m}^3$

Kurtosis = $11.11 \mu\text{gr}/\text{m}^3$

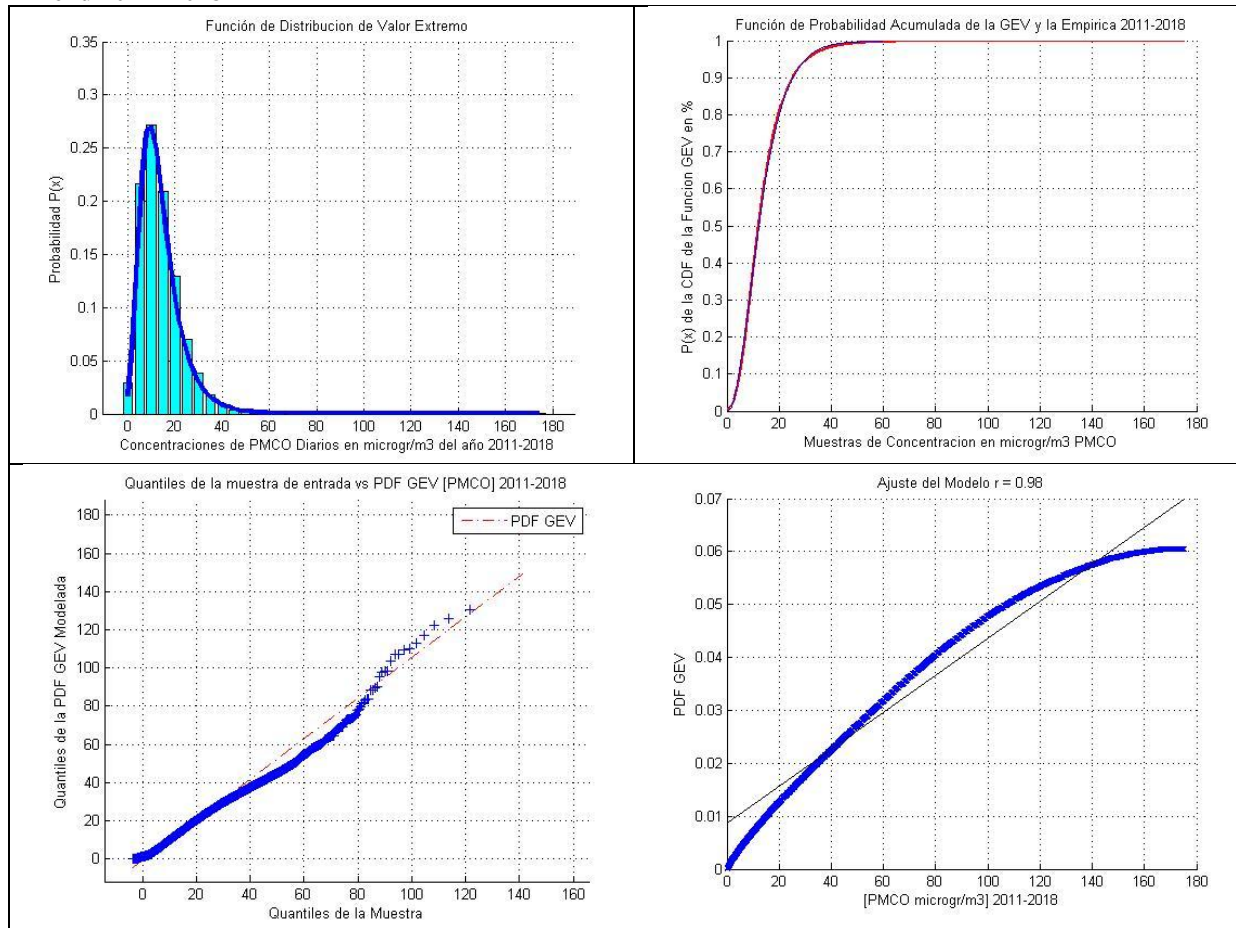
Skewness = 1.67 (Symmetry +) $\mu\text{gr}/\text{m}^3$

Gama Adjustment Trend 2011-2018

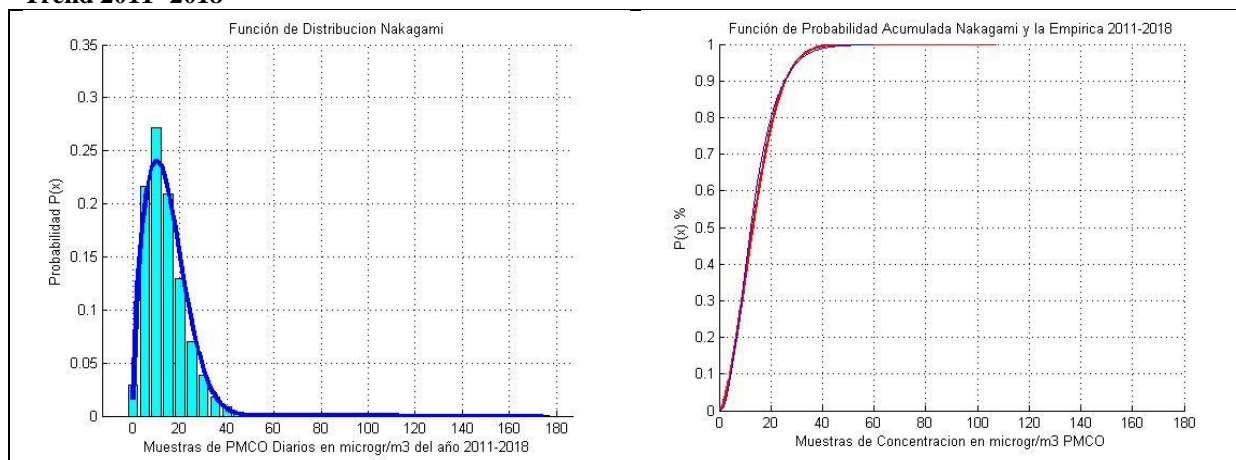




GEV Adjustment Trend 2011- 2018



Nakagami Adjustment Trend 2011- 2018



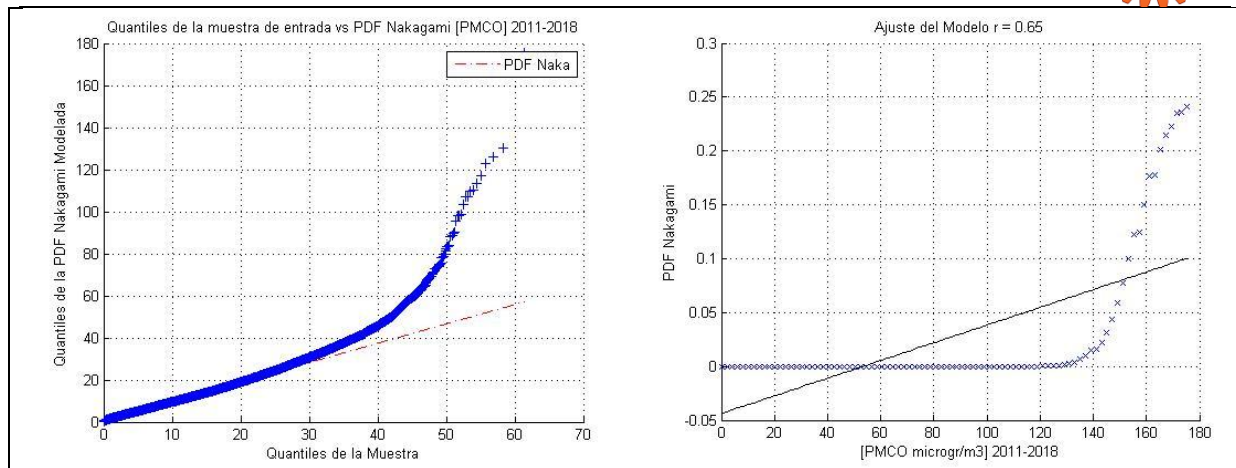


Table 3. Estimation Parameters and Trend Adjustment Indicators 2011-2018

PDF	Parameters	Adjustment Parameters	Tests of Goodness	Mean and Variance
GEV	K 0.0935 Sigma 6.1004 Mu 9.8310	RMSE = 0.4871 AP = 5.62 R2 = 0.7500 ÍA = 0.5703	Chi Test h = 0 p = 0.2807 KS Test 0	Me = 13.97 $\mu\text{gr}/\text{m}^3$ Va = 81.01 $\mu\text{gr}/\text{m}^3$
Gama	Alfa 2.6329 Beta 5.3019	RMSE = 0.4854 AP = 5.578 R2 = 0.7549 ÍA = 0.5752	Chi Test h = 0 p = 0.8046 KS Test 0	Me = 13.95 $\mu\text{gr}/\text{m}^3$ Va = 74.01 $\mu\text{gr}/\text{m}^3$
Nakagami	Mu 0.8063 Omega 271.55	RMSE = 0.5010 AP = 5.802 R2 = 0.7365 ÍA = 0.5613	Chi Test h = 0 p = 0.3541 KS Test 0	Me = 14.21 $\mu\text{gr}/\text{m}^3$ Va = 69.41 $\mu\text{gr}/\text{m}^3$

The best fit

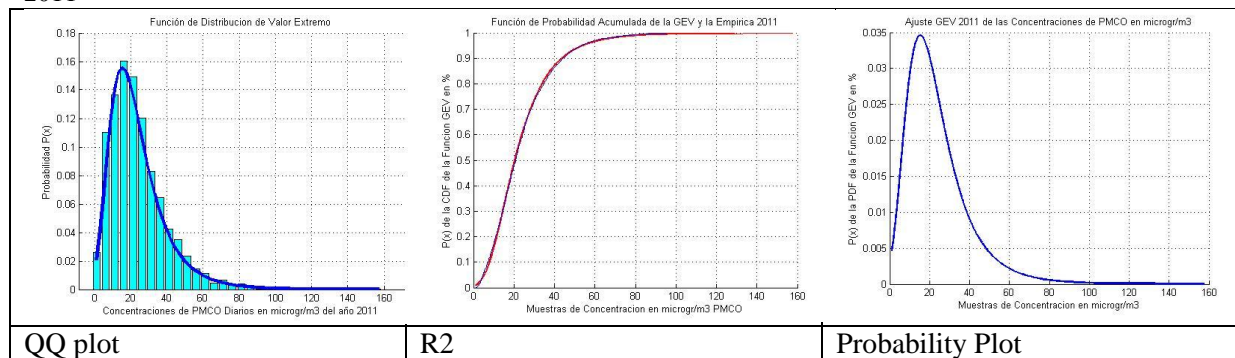
GEV data for each year

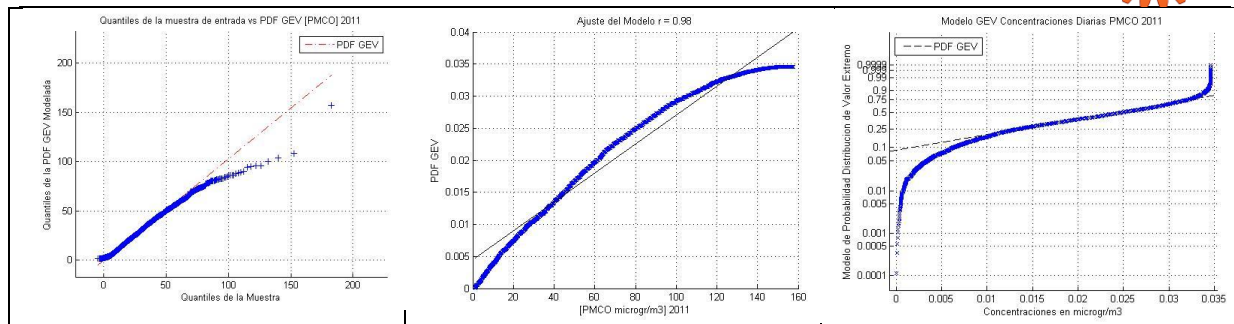
Year	GEV	Adjustment Parameters	Tests of Goodness	Mean and Variance
2011	K 0.1091 Sigma 10.6919 Mu 16.4203	RMSE = 0.4062 AP = 2.94 R2 = 0.8635 ÍA = 0.7102	Chi Test h = 0 p = 0.9469 KS Test 5.6015e-05	Me = 23.87 $\mu\text{gr}/\text{m}^3$ Va = 262.79 $\mu\text{gr}/\text{m}^3$
2012	K 0.0706 Sigma 9.1679 Mu 15.9337	RMSE = 0.4506 AP = 3.8342 R2 = 0.8078 ÍA = 0.6400	Chi Test h = 0 p = 0.5945 KS Test 0	Me = 21.91 $\mu\text{gr}/\text{m}^3$ Va = 169.62 $\mu\text{gr}/\text{m}^3$
2013	K 0.0931 Sigma 9.8987	RMSE = 0.4822 AP = 5.4869	Chi Test h = 0	Me = 22.87



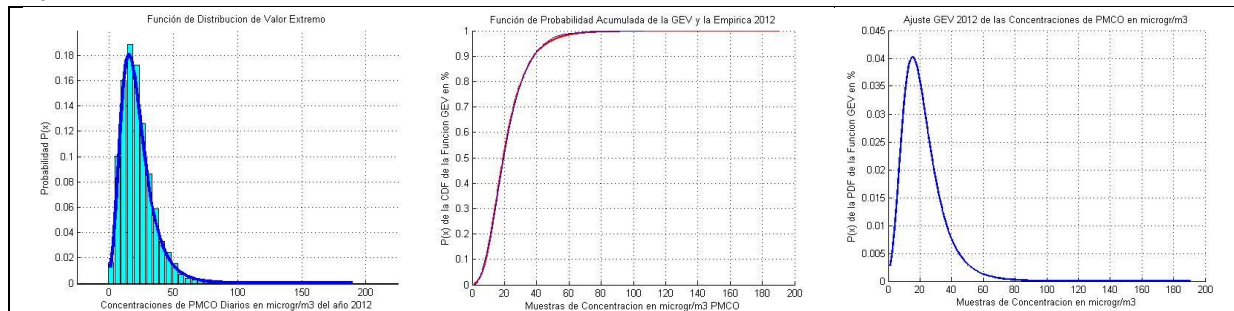
	Mu 16.1627	R2 = 0.7592 ÍA = 0.5785	p = 0.5236 KS Test 0	$\mu\text{gr}/\text{m}^3$ Va = 212.97 $\mu\text{gr}/\text{m}^3$
2014	K 0.1667 Sigma 8.4725 Mu 12.5087	RMSE = 0.3785 AP = 2.4830 R2 = 0.8854 ÍA = 0.7496	Chi Test h = 0 p = 0.6118 KS Test 0.0015	Me = 19.05 $\mu\text{gr}/\text{m}^3$ Va = 206.695 $\mu\text{gr}/\text{m}^3$
2015	K 0.0430 Sigma 5.8258 Mu 10.8859	RMSE = 0.4519 AP = 3.688 R2 = 0.8036 ÍA = 0.6405	Chi Test h = 0 p = 0.8066 KS Test 0	Me = 14.50 $\mu\text{gr}/\text{m}^3$ Va = 62.92 $\mu\text{gr}/\text{m}^3$
2016	K 0.1022 Sigma 6.1717 Mu 10.5008	RMSE = 0.4485 AP = 3.8594 R2 = 0.8121 ÍA = 0.6433	Chi Test h = 0 p = 0.1668 KS Test 0	Me = 14.75 $\mu\text{gr}/\text{m}^3$ Va = 85.45 $\mu\text{gr}/\text{m}^3$
2017	K 0.0966 Sigma 6.8770 Mu 10.6697	RMSE = 0.3933 AP = 2.5389 R2 = 0.8716 ÍA = 0.7316	Chi Test h = 0 p = 0.3565 KS Test 1.8106e-04	Me = 15.36 $\mu\text{gr}/\text{m}^3$ Va = 104.04 $\mu\text{gr}/\text{m}^3$
2018	K 0.0842 Sigma 6.4432 Mu 9.9452	RMSE = 0.3738 AP = 2.3642 R2 = 0.8905 ÍA = 0.7577	Chi Test h = 0 p = 0.0513 KS Test 4.0907e-04	Me = 14.24 $\mu\text{gr}/\text{m}^3$ Va = 87.59 $\mu\text{gr}/\text{m}^3$

Graphics of each year 2011





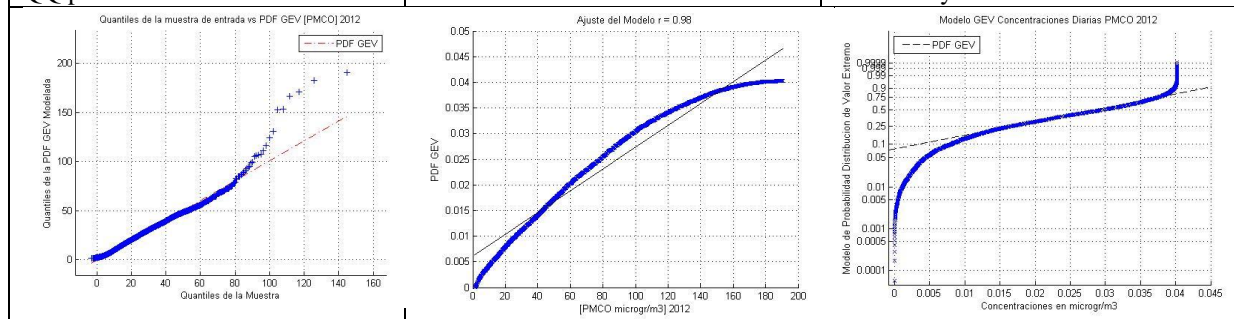
2012



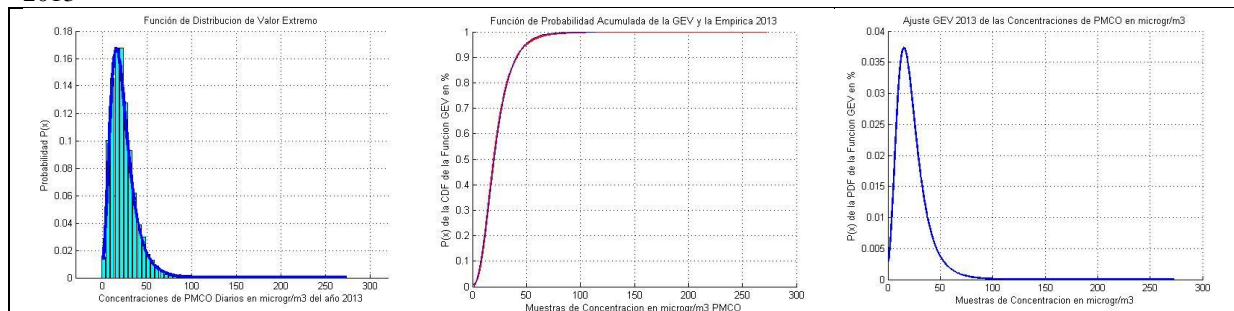
QQ plot

R2

Probability Plot



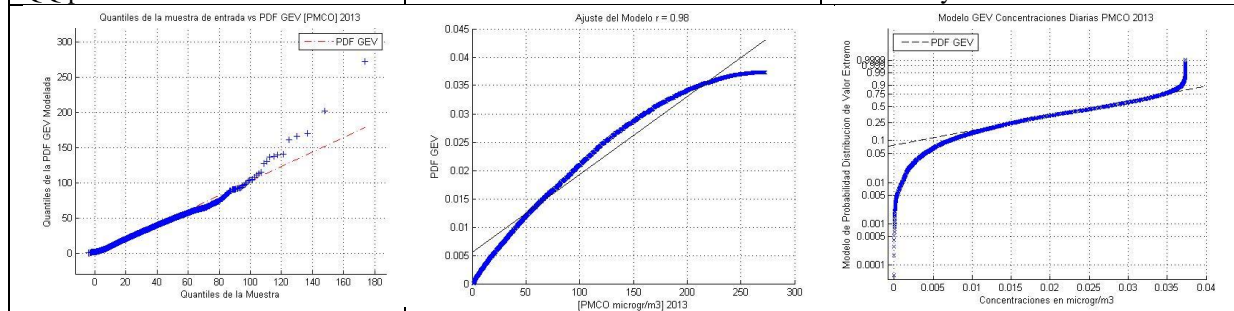
2013



QQ plot

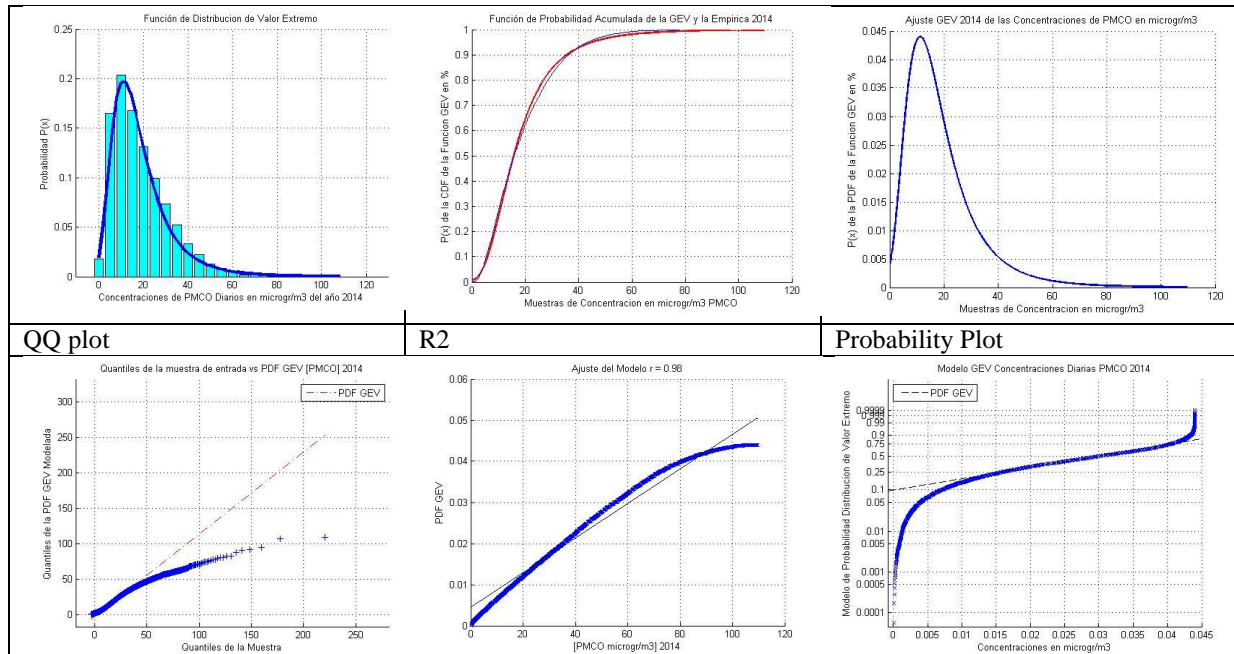
R2

Probability Plot

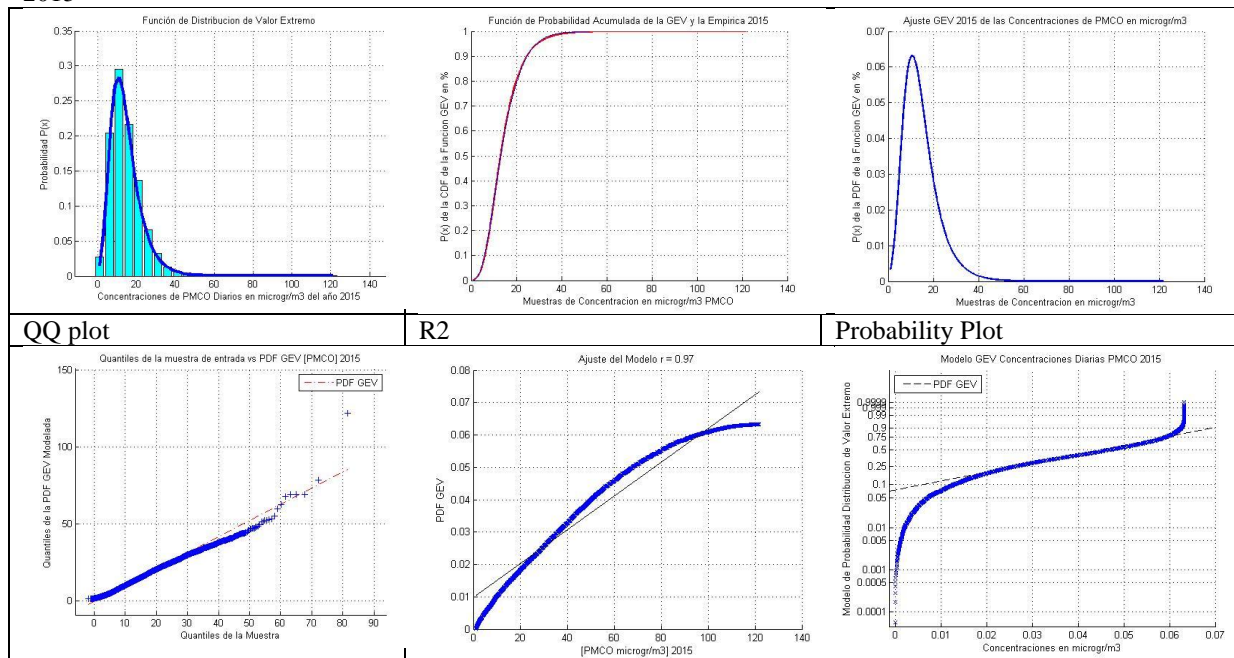




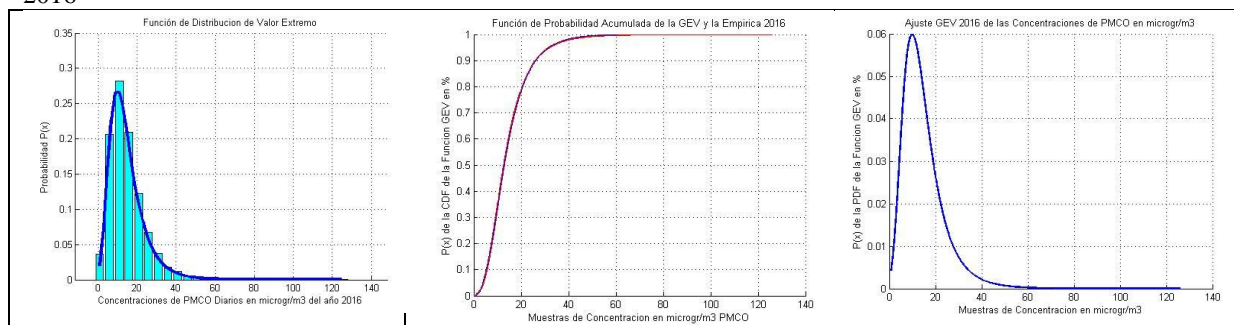
2014

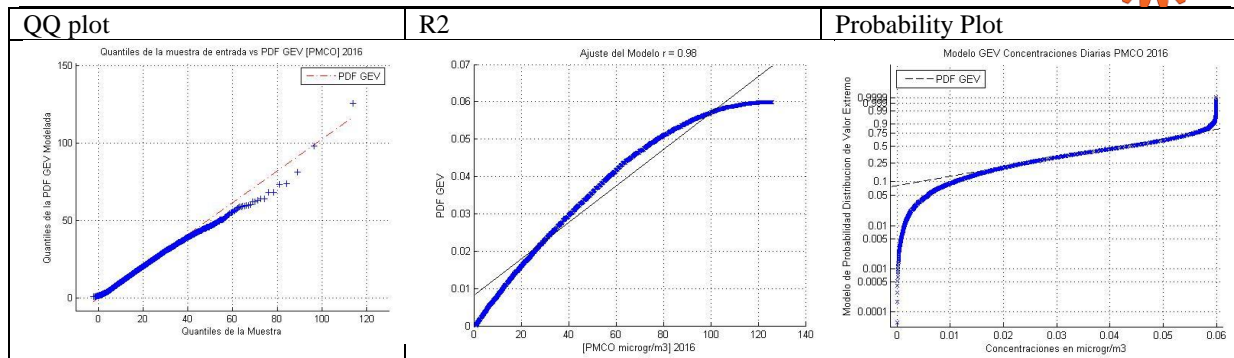


2015

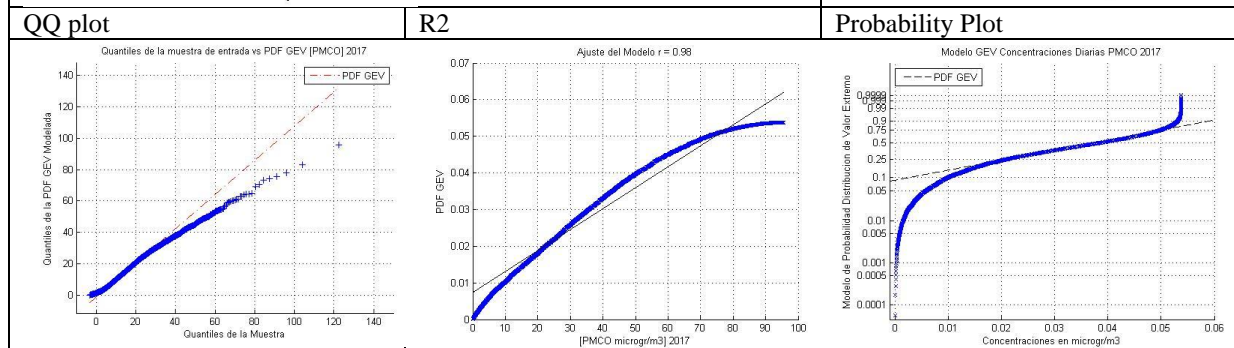
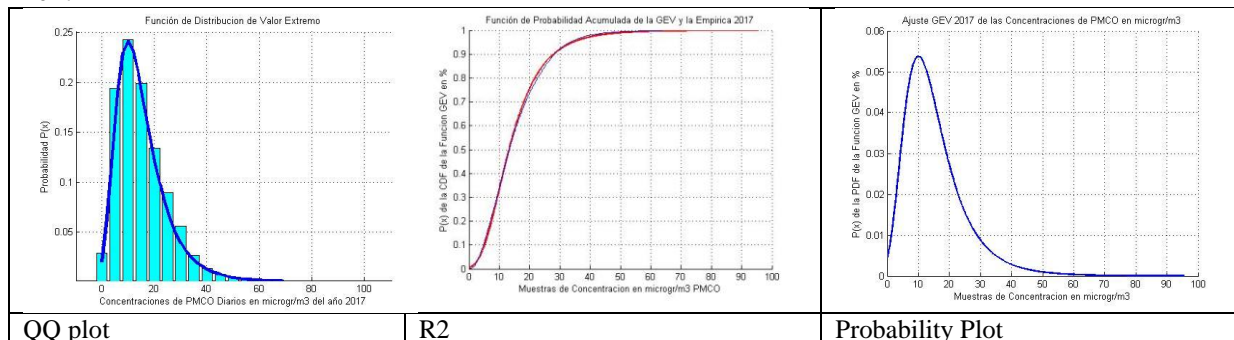


2016

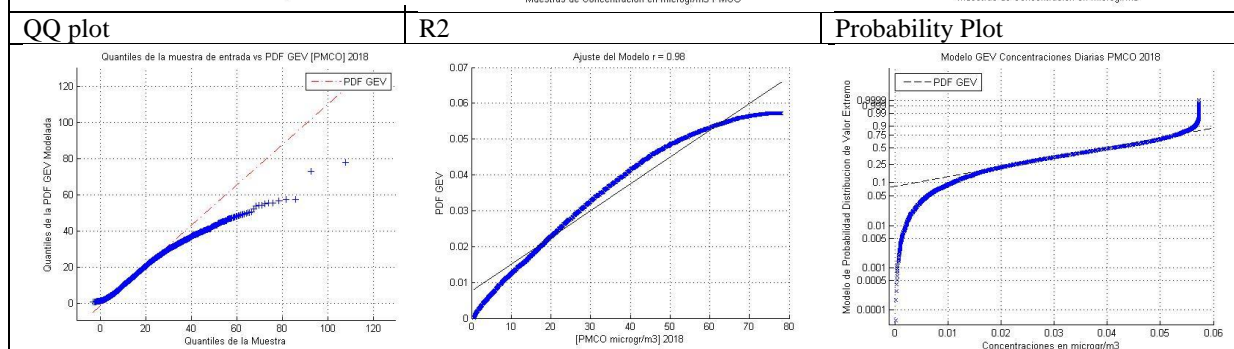
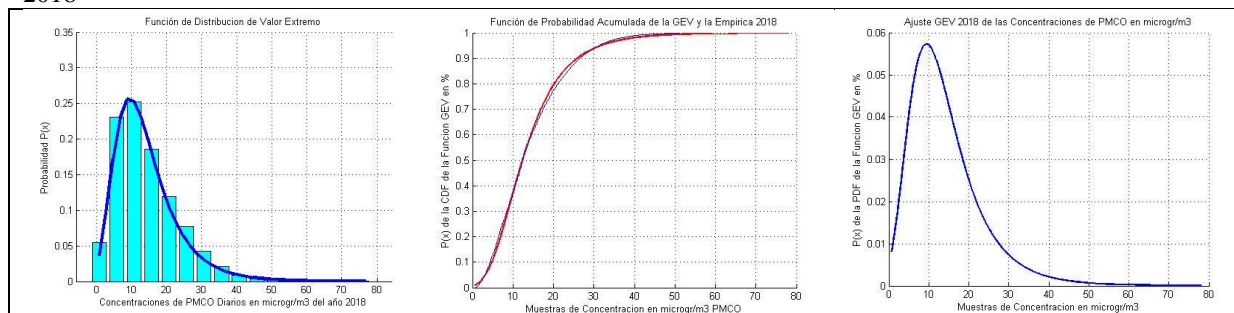




2017



2018





Now let's look at the trend this Coarse Particulate in Mexico City

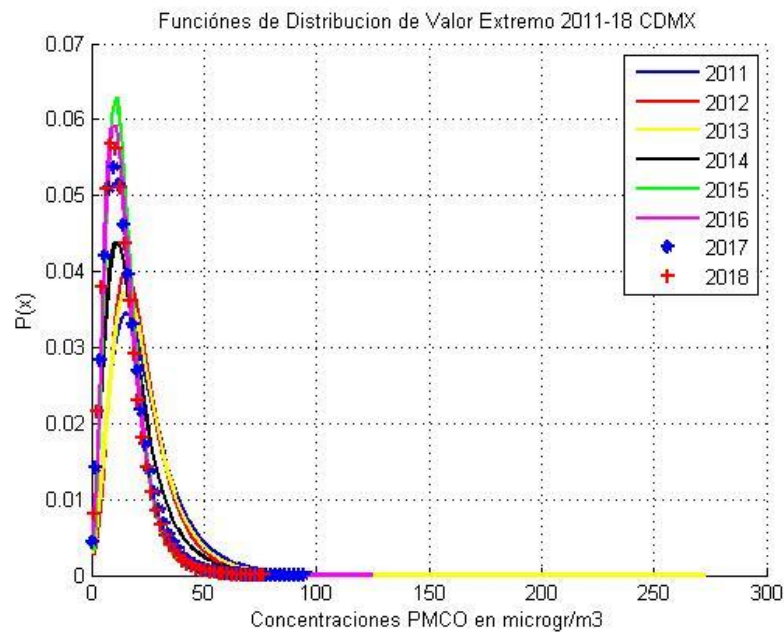


Figure 6.GEV function of each year

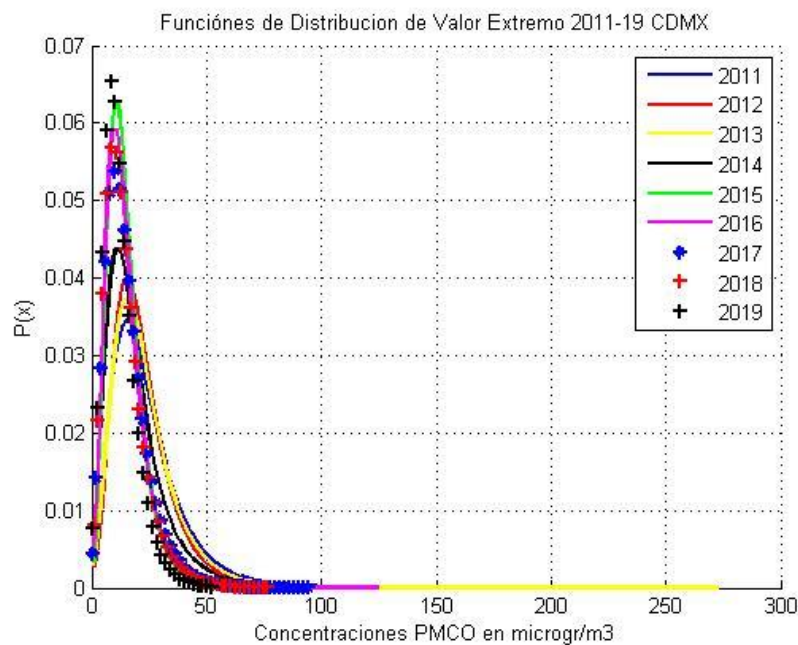
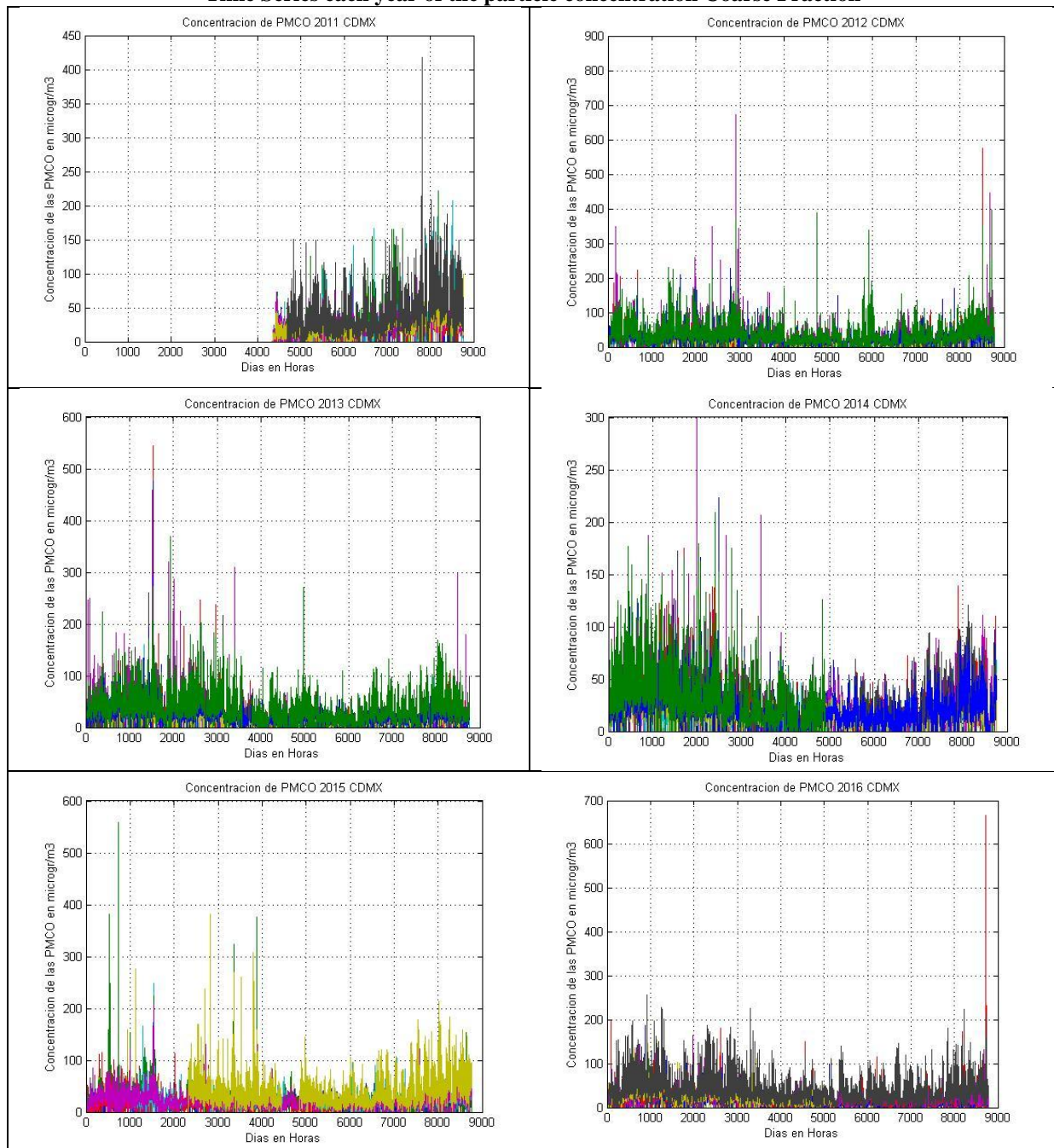


Figure 7.GEV function of each year until August 2019



Time Series each year of the particle concentration Coarse Fraction



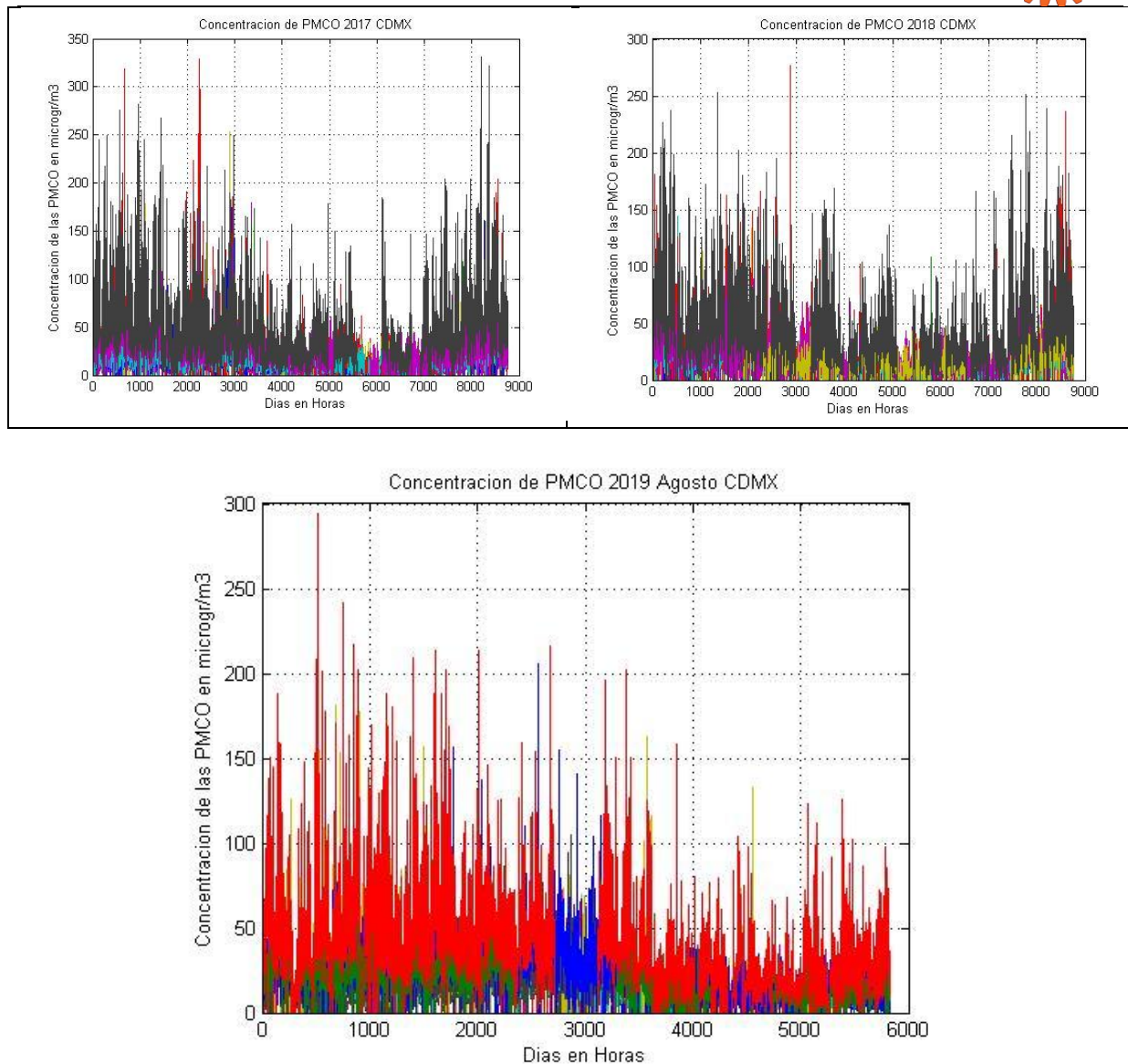


Figure 8. Temporary Serie PMCO Concentration from January to August 2019

Bayesian Point Change Detection

The Algorithm used to observe the greatest changes in the time series of PMCO concentrations in Mexico City, only from the last year, since they are daily data the number of iterations is too large, so it can only be done with The data for each year, here only shows the series of this year 2019 until August, you can see the relationship of the change that happens at a certain time of the year and the probability decreases. The change points are abrupt variations in the generative parameters of a sequence of data, the Average obtained with which it is used for the Adjustment was used.

The Bayesian Online Changepoint Detection see [12] describes an algorithm to locate those points. The algorithm uses Bayesian reasoning, and is online in the sense that it works by reading one data point at a time and providing estimates of the probability of a change point at a given time based solely on information up to that point in time. .

The approach is to imagine that the data appears in intervals or executions and that within each execution the results are i.i.d. At a point of change, the distribution changes and produces a new sequence of i.i.d variables from that distribution. The length of the execution is a random variable, and it is assumed that the distributions within an execution come from a single exponential family. For example, the distributions can be normal (with a change in mean and variance at the transition points) or poisson (with a change in the rate).



The idea behind the algorithm is that, as we read a new data, that data comes from the same distribution and the length of the execution increases by one; or that data represents a point of change, in which case the execution length is reset to zero. If the execution length increases by one, the new data provides information to improve our estimation of the parameters of the current distribution using Bayes' theorem; or, if the execution length is reset to zero, we set the distribution back to a pre-selected initial distribution and start updating its parameters based on the new data.

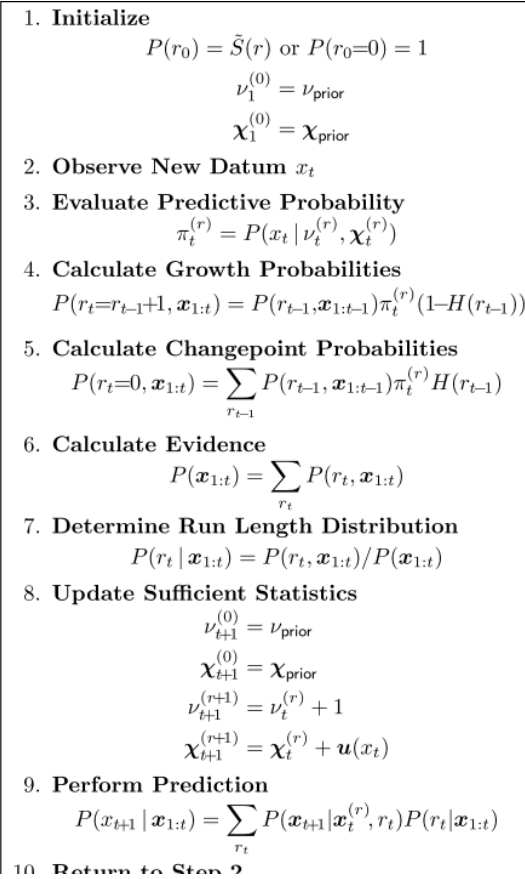


Figure 9. AlgorithmSteps

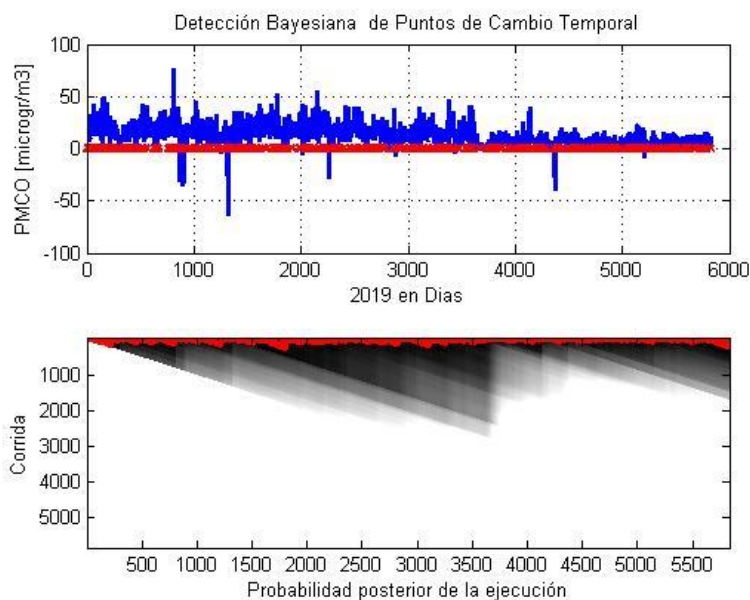


Figure 10. Probability of the PMCO Concentration until August 2019



With this algorithm we can observe the behavior of the concentrations of this Particulate, we don't have a measure, threshold or norm to be able to say if it is increasing or decreasing.

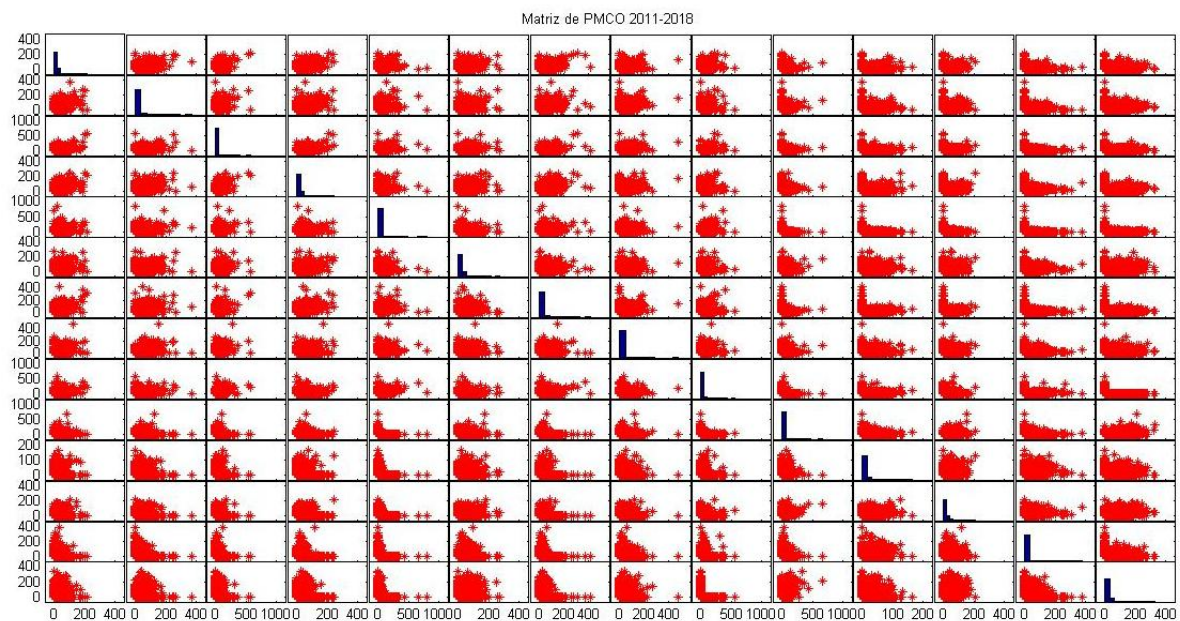


Figure 11. Graphic Matrix of the 2011-2018 PMCO Serie
A scatter plot matrix.

Conclusions

With this preliminary study, it was proved that the type of probability distribution function that was most suitable for the behavior of PMCO daily data Coarse Fraction Particles which were the best fit with the GEV pdf and the Gama pdf, this contributes to The statistics of this other pollutant that is in the Particulate category and its behavior in several cities of the world must also be monitored and monitored. This case is that of Mexico City, which does not have said primary statistical study, according to the GEV pdf we can observe a decrease of these particles in what this trend goes.

Also when applying the Bayesian Point Change Detection algorithm we can observe the greatest variations that the trend had so far this year 2019 to be able to give us an idea of the most notable changes and corroborate the time series.

References

- [1]. Aiken A. C., S. D. (2009). México City Aerosol Análisis during MILAGRO using High Resolution Aerosol Mass Spectroscopy at the Urban Supercite.
- [2]. Borja Aburto V. H., Rosales Castillo J. A., Torres Mesa V. M., Corey G. (2000). "Evaluación of Health Effects of Pollutions" Ancillary Benefits and Costs of Greenhouse Gas Mitigación. Proceedings of an IPCC Co-Sponsored Workshop.
- [3]. Data base of PMCO website of México City <http://www.aire.cdmx.gob.mx/>
- [4]. EPA (2009) "Integrated Science Assessment for Particulate Matter"
- [5]. Georgopoulos, P.G. and Seinfeld, J.H. (1982) 'Statistical distribution of air pollutant concentration', Environmental Science Technology, Vol. 16, pp.401A–416A.
- [6]. Gumbel, E.J., 1958. Statistics of Extremes. Columbia University Press, New York, p. 164.
- [7]. Kao, A. S. and Friedlander, S. K. (1995) Frequency distributions of PM10 chemical components and their sources. Environmental Science and Technology. 29(5), 19 – 28
- [8]. Lu, H., Fang, G., 2003. Predicting the exceedances of a critical PM10 concentration – a case study in Taiwan. Atmospheric Environment 37, 3491–3499.
- [9]. Organización Mundial de la Salud (2018). Calidad del Aire. Boletín del 2 de Mayo del 2018. Secretaría del Medio Ambiente de la Ciudad de México en el Inventario de Emisiones de la Ciudad de México 2016.
- [10]. Otten, A., and M. A. J. Van Montfort, Maximum-likelihood estimation of the general extreme-value distribution parameters, J. Hydrol., 47, 187–192, 1980.



- [11]. Prescott, P., and A. T. Walden, Maximum-likelihood estimation of the parameters of the three-parameter generalized extreme-value distribution from censored samples, *J. Stat. Comput. Simul.*, 6, 241–250, 1983.
- [12]. Ryan P. Adams, David J.C. MacKay, Bayesian Online Changepoint Detection, arXiv 0710.3742 (2007) Bayesian Online Changepoint Detection, Ryan Prescott Adams, David J.C. MacKay <https://arxiv.org/abs/0710.3742>
- [13]. P.G. Georgopoulos, J.H. Seinfeld, Statistical distributions of air pollutant concentrations, *Environ. Sci. Technol.*, 16 (1982) 401A-416A.
- [14]. Roberts, E.M., 1979. Review of statistics of extreme values with applications to air quality data, part II. Applications. *Journal of Air Pollution Control Association* 29, 733–740.
- [15]. Samet, J., Domonici, F., Curriero, F.C., Coursac, I. and Zeger, S.L. (2000) 'Fine particulate air pollution and mortality in 20 US cities', *New England Journal of Medicine*, Vol. 343, pp.1742–1749.
- [16]. SEMARNAT, Dirección General de Gestión de la Calidad del Aire y Registro de Emisiones y Transferencia de Contaminantes en conjunto con el Instituto Nacional de Ecología. *Inventario Nacional de Emisiones 2008*.
- [17]. Xuan Xiang, Kevin Murphy, Modeling Changing Dependency Structure in Multivariate Time Series, *ICML (2007)*, pp. 1055—1062
- [18]. Zenteno Jiménez José Roberto, Prediction of Concentrations of Ozone Levels in México City using Probability Distribution Functions, *International Journal of Latest Research in Engineering and Technology (IJLRET)* // Volume 04 - Issue 07 // July 2018 // PP. 35-45
- [19]. Zenteno Jiménez José Roberto. A Methodology for Obtaining new Probability Distributions Functions Normal and Extreme Value for Bayesian Inference and Stochastic Mixed Gaussian Case One: For Daily Concentration Data Maximum Ozone. *International Journal of Latest Research in Engineering and Technology (IJLRET)* // Volume 04 - Issue 11 // November 2018 // PP. 15-35
- [20]. Zenteno Jiménez José Roberto, Prediction of Concentrations of Suspended Particle Levels of 10 micrometers (PM10) in México City with Probability Distribution Functions, *Trend 2010-2018. International Journal of Latest Research in Engineering and Technology (IJLRET)* www.ijlret.com // Volume 05 - Issue 04 // April 2019 // PP. 01-19
- [21]. Zenteno Jiménez José Roberto, Prediction of Concentrations of Suspended Particle Levels of 2.5 micrometers (PM2.5) in Mexico City with Probability Distribution Functions and its Trend, *International Journal of Latest Research in Engineering and Technology (IJLRET)* www.ijlret.com // Volume 05 - Issue 04 // April 2019 // PP. 01-17